Optimizing Itinerary Selection and Charging Association for Mobile Chargers

Sheng Zhang, *Member, IEEE*, Zhuzhong Qian, *Member, IEEE*, Jie Wu, *Fellow, IEEE*, Fanyu Kong, and Sanglu Lu, *Member, IEEE*

Abstract—Wireless power transfer provides a promising way to extend the battery lifetime of our energy-hungry rechargeable devices. Previous studies have envisioned using mobile vehicles/robots/drones equipped with high capacity batteries as mobile chargers to replenish those devices, and they mainly focus on maximizing network lifetime, optimizing efficiency of charging scheduling, minimizing total charging delay, etc. However, existing methods may be insufficient and inflexible when the energy consumption of rechargeable devices fluctuates over time, or when rechargeable devices are sparse. In this paper, we consider how to efficiently provide flexible wireless charging using pre-planned charging itineraries. We present the Itinerary Selection and Charging Association (ISCA) problem: given a set of rechargeable devices and a set of candidate charging itineraries, how can we select itineraries and determine a corresponding charging association to minimize the amount of energy which is due to mobile chargers' movement and wireless charging loss, so that every device gets its required energy. We prove that ISCA is NP-complete by reducing the set cover problem to it. We start solving this problem by first looking at the case in which an itinerary can only be used once, and we propose an algorithm with approximation ratio of $O(\ln M)$ and a practical heuristic algorithm, where M is the number of devices. For the general case in which an itinerary may be used multiple times, we propose an approximation algorithm of factor 10 using the Primal-Dual schema. Evaluations results from real field experiments and extensive simulations show that the proposed algorithms have near-optimal performance and PDA reduces the amount of wasted energy by up to 65 percent compared with a set cover-based algorithm.

Index Terms—Wireless power transfer, approximation algorithm, Primal-Dual schema

1 Introduction

Wireless devices have greatly improved the overall quality of life over the past few years. Because they are battery-powered they remain operational only for a limited amount of time before connecting to wired chargers. To extend the lifetime of these energy-hungry devices, and thus enhance their usability, various approaches from different perspectives have been proposed, including energy harvesting [1], which extracts energy from the environment (e.g., solar, wind, and vibration), energy conservation [2], which focuses on slowing down the energy consumption rate and battery replacement [3]. However, energy harvesting remains limited in practice due to its partial predictability and the relatively large size of harvesting panels; energy conservation cannot compensate for depletion; battery replacement is costly and impractical.

Recently, Kurs et al. [4] experimentally demonstrated that energy can be efficiently transmitted between magnetically resonant objects without any interconnecting conductors, e.g., powering a 60 W light bulb, which is two meters away, with approximately 40 percent efficiency. Kang et al. [5] experimentally demonstrated that rechargeable lithium batteries can have high energy densities and high charge/discharge capabilities. These two technologies together provide a promising paradigm to extend the battery lifetimes of our daily-use devices and have led to the development of several commercial products. 30+ kinds of popular phones are beginning to embrace wireless charging [6], and even vehicles [7] and unmanned planes [8] are now supporting wireless charging. It is predicted that this market will be worth $13.78 billion by 2020 [9].

With these enabling technologies, existing studies [10], [11], [12], [13], [14], [15] proposed periodically employing static or mobile chargers to replenish rechargeable devices, such as RFID tags, sensors, smartphones, tablets, and cars, for the purpose of maximizing the lifetime of the underlying network [10], optimizing the efficiency of charging scheduling [11], [12], minimizing total charging delay [13], etc. Most of these studies fit comfortably under one of two headings: *stationary deployment* [15], [16], [17], which focuses on optimizing the deployment of fixed chargers, or *mobile charging* [10], [11], [12], [13], [14], [18], [19], [20], which focuses on optimizing charging sequence and/or duration. However, as we will explain in Section 3, existing methods may be insufficient and inflexible when the energy consumption of rechargeable devices fluctuates over time or when rechargeable devices are sparse.

We observed that in some applications (e.g., underwater monitoring and agricultural rain-fed farming), rechargeable devices are deployed in environments that prohibit the

- *S. Zhang, Z.Z. Qian, and S.L. Lu are with the State Key Laboratory for Novel Software Technology, Nanjing University, Nanjing 210023, China. E-mail: {sheng, qzz, sanglu}@nju.edu.cn.*
- *J. Wu is with the Department of Computer and Information Sciences, Temple University, Philadelphia, PA 19122. E-mail: jiewu@temple.edu.*
- *F.Y. Kong is with Ant Financial, China. E-mail: njukongfy@gmail.com.*

Manuscript received 22 Apr. 2016; revised 10 Nov. 2016; accepted 12 Dec. 2016. Date of publication 19 Dec. 2016; date of current version 29 Aug. 2017. For information on obtaining reprints of this article, please send e-mail to: reprints@ieee.org, and reference the Digital Object Identifier below. Digital Object Identifier no. 10.1109/TMC.2016.2641446

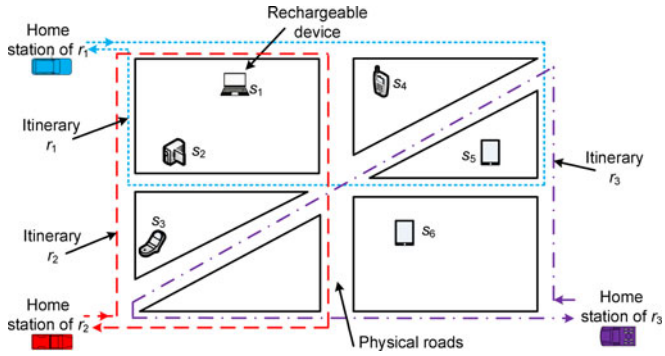

Fig. 1. Mobile charging with fixed candidate itineraries.

approach of mobile chargers, i.e., mobile chargers can only travel along existing infrastructures, e.g., bridges and roads. This motivates us to propose a new charging paradigm: *charging with fixed candidate itineraries*. A charger could be integrated with a bus or some other moving tool that travels along a fixed path into a single entity, which would make it easy to deploy and install. Specifically, we want to provide wireless charging service in a two-dimensional (2-D) target area. Based on historical data analysis and investigation, we can predict the locations of potential rechargeable devices, and then preselect a number of candidate itineraries. These itineraries are used by mobile chargers to deliver energy to rechargeable devices. Each mobile charger starts from the home station of an itinerary with a limited battery [11], [12], travels along the itinerary, transfers energy to some devices, and finally, returns to the home station for battery replenishment or replacement [21]. Fig. 1 shows an example consisting of three itineraries and six rechargeable devices.

Wireless power transfer is not perfect, i.e., there is energy loss when a mobile charger transfers energy to a device. Furthermore, the movement of each charger also costs energy. Therefore, the energy consumed in the system can be classified into three types: *loss-energy*, which varies depending on charging distance and duration, *movement-energy*, which is used by mobile chargers for moving, and *payload-energy*, which is eventually received by rechargeable devices. Given a fixed payload-energy, the goal of this paper is to minimize the sum of movement-energy and loss-energy. To achieve this, we must strategically select a subset of the candidate itineraries (i.e., *itinerary selection*) and determine which itinerary is responsible for charging each device (i.e., *charging association*).

The Itinerary Selection and Charging Association (ISCA) problem can be briefly stated as follows: Given a set of rechargeable devices and a set of candidate charging itineraries, we question how to find an itinerary selection and a corresponding charging association solution to minimize the sum of movement-energy and loss-energy so that every device gets its required energy. In this paper, we prove that this problem is NP-complete by a reduction from the set cover problem [22]. For the case in which an itinerary can only be used once, we propose an $O(\ln M)$-approximation algorithm and a practical heuristic algorithm, where M is the number of rechargeable devices; for the general case in which an itinerary may be used multiple times, we propose an approximation algorithm of factor 10 based on the Primal-Dual schema.

To the best of our knowledge, we are the first to propose mobile charging with candidate itineraries. We evaluate the proposed algorithms using both real field experiments and extensive simulations. We summarize our contributions here as follows.

- We identify the itinerary selection and charging association problem and prove that it is NP-complete.
- We design approximation algorithms and efficient heuristics for both ISCA and ISCA-MP.
- Real field experiments and extensive simulations are conducted to confirm our theoretical findings.

The remainder of the paper is organized as follows. We discuss related work in Section 2. We motivate our problem and give its formulation in Section 3. We present the algorithms to ISCA and ISCA-MP in Sections 4 and 5, respectively. Field experiments and extensive simulations are presented in Sections 6 and 7, respectively. We conclude the paper in Section 8.

2 Related Work

Since its inception, wireless power transfer has attracted much attention. Existing studies can be classified into two broad types: stationary and mobile chargers.

For stationary chargers, He et al. [16] proposed point and path provisioning for charger placement based on the Intel wireless identification and sensing platform. Tong et al. [23] found that a charger can transfer energy to multiple devices simultaneously without significantly reducing the received energy at each device. Zhang et al. [15] considered charger placement with adjustable power levels and power budget. Dai et al. [17] studied how to obtain the maximum electromagnetic radiation point under a given charger placement. Radiation safety and capacity restrictions are taken into account in [24], [25].

For mobile chargers, existing studies have considered various decision variables and objectives. To maximize network lifetime, charging sequence and packet routing are optimized in [10], [18], while Shu et al. [26] optimized the same objective under varying charger velocities. To maximize the ratio of the charger's vacation time (i.e., time spent at the home service station) over the cycle time, travelling path and stop schedules are optimized in [11], [12]. Fu et al. [13] optimized the charger stop locations and durations for minimizing the total charging delay of all sensors. Wang et al. [21] proposed NDN-based energy monitoring and reporting protocols with a special focus on scheduling mobile chargers for multiple concurrent emergencies. Zhang et al. [14] utilized collaboration between mobile chargers to improve the energy usage effectiveness. To simultaneously minimize charger travel distance and charging delay, He et al. [19] proposed synchronizing charging sequences based on multiple nested tours, and Fu et al. [27] employed the same technique to simultaneously minimize charger travel distance and charging delay. Given the heterogenous charging frequencies of sensors, scheduling multiple charging rounds to minimize total moving distance of mobile chargers is studied in [28]. Nikoletseas et al. [29] proposed the peer-to-peer interactive charging problem where mobile entities are both energy transmitters and harvesters.

Wang et al. [30] designed a hybrid framework which combines solar energy harvesting for cluster heads and wireless charging for normal sensor nodes. Chen et al. [31] investigated the problem of maximizing the number of nodes a path can charge within a given budget (e.g., in terms of time, energy).

In contrast, we focus on employing mobile chargers with fixed candidate itineraries to periodically replenish rechargeable devices with the goal of minimizing unnecessary energy wasted, i.e., movement-energy and loss-energy.

The optimization techniques are inspired by two optimization problems, e.g., vehicle routing problem (VRP) [32] and facility location problem (FLP) [33]. Given a road network, VRP is to find the optimal itineraries for multiple vehicles to traverse so that a given set of customers are delivered. FLP is to find the optimal placement of facilities to minimize transportation costs. Although their solutions greatly inspired us, ISCA differs from them in two main aspects: (a) the cost of an itinerary in ISCA is determined by not only its length, but also by the devices that will be charged by the itinerary and (b) ISCA will simultaneously select a subset of given itineraries and decide the association relationship between itineraries and devices.

3 Motivation and Problem

3.1 Motivation

Wireless power transfer has been studied extensively because of its wide use in recent years. It can be used to periodically deliver energy to rechargeable wireless sensor networks and can also facilitate the charging of our daily-use tools like electric toothbrushes and vacuum cleaner robots. In these application scenarios, we may wish that we can use wireless charging just like cellular networks. In fact, this can be achieved by deploying multiple fixed wireless chargers to cover an area of interest. However, this method may be insufficient in the scenarios below:

- *Bursty demands*. The number of rechargeable devices and/or the energy consumption of these devices may fluctuate over time. If we place a number of fixed chargers, they may be unable to satisfy the bursty demands for charging.
- *Sparse devices*. There may be not always many devices within the area of interest. For areas with sparse devices, deploying fixed chargers may be not cost-efficient; instead, mobile chargers with carefully planned itineraries could be appropriate.
- *Service decoupling*. In the future, there may be many charging service providers that compete with each other. Each service provider will have several charging itineraries passing through the area of interest. We may want to choose some of these itineraries to meet the charging demands while minimizing the wasted energy.

Therefore, we propose delivering energy to an area via mobile chargers which follow pre-defined itineraries. Our tasks are to select a subset of these itineraries and to determine the association between selected itineraries and rechargeable devices. This method is flexible: when there are bursty energy demands, we can arrange more chargers; when a target area contains very few devices, we can arrange chargers less frequently.

3.2 Charging Model and Itinerary

We consider a network composed of M stationary rechargeable devices, denoted by the set $\mathcal{S} \triangleq \{s_i\}_{i=1}^{M}$ and distributed in a two-dimensional plane. The energy requirement of each device is E, i.e., when a mobile charger transfers energy to a device, the device must receive E units of energy.

In some applications, rechargeable devices are deployed in environments that prohibit the approach of mobile chargers. Mobile chargers can only travel along existing infrastructures like bridges and roads. Besides, a charger could be integrated with a bus or some other moving tool, which travels along a fixed path, into a single entity, making it easy to deploy and install. Therefore, we assume that there is a set of N candidate charging itineraries, denoted by the set $\mathcal{R} \triangleq \{r_i\}_{i=1}^{N}$. Without causing confusion, we also use r_i to denote the mobile charger that travels along itinerary r_i.

A mobile charger r_i has a limited battery with capacity B_i. When a charger transfers energy to a device, the charger's transmission power is P. Thus, the charging capacity of r_i, in terms of charging time, can be denoted by

$$T_i = B_i/P. \tag{1}$$

We consider that the movement of each charger is supported by petrol,[1] and we assume the amount of movement-energy along itinerary r_i, denoted by c_i, is dictated by the physical length of r_i.

We assume an omnidirectional wireless power transfer model in which the amount of received power at each device is only dominated by the transmission power of the charger and the distance between them. As indicated by the experiments in [16], the power p_{ij} received by device s_j from charger r_i can be quantified by an empirical model as follows:

$$p_{ij} = \begin{cases} \frac{aP}{(d_{ij}+b)^2} & d_{ij} \le D, \\ 0 & d_{ij} > D. \end{cases} \tag{2}$$

Here, constants a and b are determined by environments and hardware of chargers and devices. d_{ij} is the physical distance between r_i and s_j. D is the maximum cover distance of each charger.[2]

We use t_{ij} to represent the time for charger r_i to charge s_j to its full requirement, i.e., s_j should obtain E units of energy after being charged by r_i. We have

$$t_{ij} = \frac{E}{p_{ij}} = \frac{E(b+d_{ij})^2}{aP}. \tag{3}$$

1. However, our formulation can be easily extended to the case in which the movement of each charger is supported by battery: just replace B_i in Eq. (1) by $(B_i - c_i)$.

2. In fact, when the transmission power P increases, D also increases. When a device is far away from a charger, the device may receive negligible power which is hard to be rectified to useful energy. Denote the threshold of this negligible power by p_{th}, then we have $D = \sqrt{aP/p_{th}} - b$. However, since P is constant in our problem, we assume D is also constant.

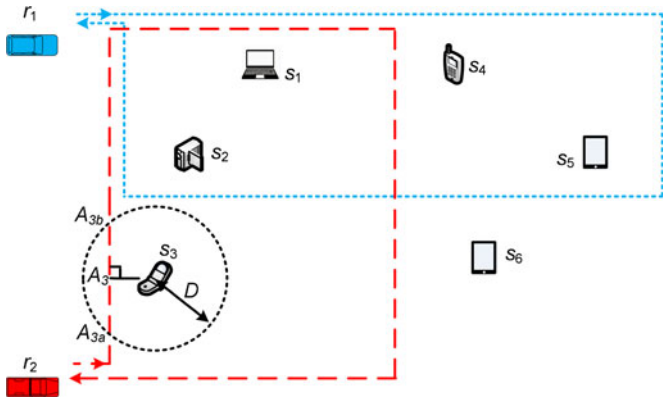

Fig. 2. Suppose that r_2 is responsible for charging s_3 when it arrives at A_{3a}. Although it could start transferring power to s_3, to minimize loss-energy, it will not begin transmitting power until it arrives at A_3, and it will stop at A_3 for a duration of t_{23} to charge s_3.

Therefore, when r_i charges s_j to its full requirement, the amount of loss-energy, denoted by f_{ij}, can be obtained as follows:

$$f_{ij} = (P - p_{ij})t_{ij} = \left(P - \frac{aP}{(d_{ij}+b)^2}\right)\frac{E(b+d_{ij})^2}{aP} = \left(\frac{(b+d_{ij})^2}{a} - 1\right)E. \quad (4)$$

We see that when E is fixed, the loss-energy f_{ij} is dictated by d_{ij}. Therefore, to minimize loss-energy, a mobile charger transmits power to a device only when it arrives the location that is closest to that device. For example, in Fig. 2, suppose that r_2 is responsible for charging s_3 when it arrives at A_{3a}. Although it could start transferring power to s_3, to minimize loss-energy, it would not begin transmitting power until it arrives at A_3, and it would stop at A_3 for a duration of t_{23} to charge s_3.

To accomplish this, as proposed in [20], [30], mobile chargers are equipped with positioning devices (e.g., GPS, gyroscope, etc) to locate themselves so that they can easily recognize the location (e.g., A_3 in Fig. 2) that is closest to each rechargeable device.

Table 1 provides a quick reference for main notations.

3.3 Problem Formulation

We use y_i to indicate whether itinerary r_i is used, and x_{ij} to indicate whether r_i is responsible for charging s_j. Then, the total energy consumed in our problem can be classified into three types: the payload-energy $E \cdot M$, the movement-energy $\sum_{r_i \in \mathcal{R}} c_i y_i$, and the loss-energy $\sum_{r_i \in \mathcal{R}} \sum_{s_j \in \mathcal{S}} f_{ij} x_{ij}$. When the payload-energy is fixed, i.e., ME, the objective of this paper is to minimize the sum of movement-energy and loss-energy, i.e.,

$$\min \quad \sum_{r_i \in \mathcal{R}} c_i y_i + \sum_{r_i \in \mathcal{R}} \sum_{s_j \in \mathcal{S}} f_{ij} x_{ij}.$$

The following constraints must be satisfied. First, every device should be covered and charged, i.e.,

$$\sum_{i \in \mathcal{R}} x_{ij} \geq 1, \quad \forall s_j \in \mathcal{S}.$$

TABLE 1
Main Notations for Quick Reference

Symbol	Meaning
$\mathcal{R}$	the set of candidate itineraries
N	the number of candidate itineraries
P	the transmission power of a charger
B_i	the battery capacity of a mobile charger r_i
$\mathcal{S}$	the set of stationary rechargeable devices
M	the number of stationary devices
E	the energy requirement of a device
r_i	a candidate itinerary or a mobile charger
c_i	the movement-energy of an itinerary r_i
T_i	the charging time capacity of an itinerary r_i
s_j	a rechargeable device
d_{ij}	the minimum distance between r_i and s_j
t_{ij}	the time for r_i to charge s_j to its requirement
f_{ij}	the loss-energy during r_i charges s_j

Second, we must guarantee that only selected itineraries (i.e., chargers) can deliver energy to devices, i.e.,

$$y_i - x_{ij} \geq 0, \quad \forall s_j \in \mathcal{S}, r_i \in \mathcal{R}.$$

We would like to mention that since ISCA is a *minimization* problem, if no devices are charged by an itinerary r_i, then y_i must be 0; therefore, it is unnecessary to add other constraints to *explicitly* make sure that $y_i = 0$ if no devices are charged by r_i.

Third, no itinerary (i.e., charger) can be overloaded, i.e.,

$$T_i y_i - \sum_{s_j \in \mathcal{S}} t_{ij} x_{ij} \geq 0, \quad \forall r_i \in \mathcal{R}.$$

We then have the Itinerary Selection and Charging Association problem:

$$\min \quad \sum_{r_i \in \mathcal{R}} c_i y_i + \sum_{r_i \in \mathcal{R}} \sum_{s_j \in \mathcal{S}} f_{ij} x_{ij} \qquad \text{[ISCA]} \quad (5a)$$

$$\text{s.t.} \quad T_i = B_i / P \qquad \forall r_i \in \mathcal{R} \quad (5b)$$

$$t_{ij} = \frac{E(b+d_{ij})^2}{aP} \qquad \forall s_j \in \mathcal{S}, r_i \in \mathcal{R} \quad (5c)$$

$$f_{ij} = \left(\frac{(b+d_{ij})^2}{a} - 1\right)E \qquad \forall s_j \in \mathcal{S}, r_i \in \mathcal{R} \quad (5d)$$

$$\sum_{i \in \mathcal{R}} x_{ij} \geq 1, \qquad \forall s_j \in \mathcal{S} \quad (5e)$$

$$y_i - x_{ij} \geq 0, \qquad \forall s_j \in \mathcal{S}, r_i \in \mathcal{R} \quad (5f)$$

$$T_i y_i - \sum_{s_j \in \mathcal{S}} t_{ij} x_{ij} \geq 0, \qquad \forall r_i \in \mathcal{R} \quad (5g)$$

$$x_{ij} \in \{0,1\}, \qquad \forall s_j \in \mathcal{S}, r_i \in \mathcal{R} \quad (5h)$$

$$y_i \in \{0,1\}, \qquad \forall r_i \in \mathcal{R} \quad (5i)$$

where Eqs. (5h) and (5i) are integral constraints. Note that Eq. (5i) will be *relaxed* to $y_i \in \mathcal{Z}^+$ in Section 5, for which we design a constant-factor approximation algorithm.

Despite our focus on itinerary selection and charging association, the generic optimization framework makes our analysis and solution applicable to a wide range of ISCA variants such as stationary charger placement and association (in this case, setting up a stationary charger may incur

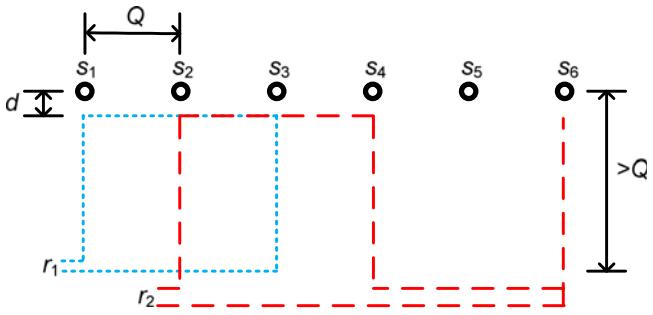

Fig. 3. Reduction from SC to ISCA. By choosing proper ds, Ds, and T_is, we can guarantee that r_i can *only* cover the devices that belong to $\mathcal{V}_i$.

a cost) and joint optimization of power allocation and data collection. These problems have a common objective of minimizing two types of costs: static cost (e.g., movement-energy) and dynamic cost (e.g., loss-energy).

3.4 Problem Hardness

Theorem 1. *The decision version of ISCA is NP-complete.*

Proof. We prove this theorem by reduction from the Set Cover problem (SC) [22], which is NP-complete. □

Definition 1 (Set Cover). *Given a universe $\mathcal{U} = \{e_1, e_2, \ldots, e_m\}$ of m elements, a collection of subsets of $\mathcal{U}$, $\mathcal{V} = \{\mathcal{V}_1, \mathcal{V}_2, \ldots, \mathcal{V}_k\}$, the cost of $\mathcal{V}_i$ is h_i, and an integer K, does there exist a sub-collection of $\mathcal{V}$, with no more than K cost, that covers all elements of $\mathcal{U}$?*

Given an instance of SC, we construct an instance of ISCA as follows. The main idea is to *carefully decide the distance d_{ij} between chargers and devices*.

We let $N = k$ and $M = m$ in ISCA, i.e., each itinerary corresponds to a subset, and each device corresponds to an element. We line up all m devices at Q distance apart (see Fig. 3). In doing so, we can arrange the itineraries as in Fig. 3 to make sure that if $e_j \in \mathcal{V}_i$, then the shortest distance d_{ij} between r_i and s_j is exactly d; otherwise, $d_{ij} > Q$. For example, in Fig. 3, if $\mathcal{V}_1 = \{e_1, e_2, e_3\}$ and $\mathcal{V}_2 = \{e_2, e_3, e_4, e_6\}$, we can arrange r_1 and r_2 as in the figure.

By choosing proper ds, Qs, and T_is, we can guarantee that the charging capacity (i.e., T_i) of r_i can cover only the devices that belong to $\mathcal{V}_i$:

$$T_i = \frac{E(b+d)^2}{aP} \cdot |\mathcal{V}_i|, \tag{6}$$

and r_i cannot charge any device that does not belong to $\mathcal{V}_i$:

$$E(b+Q)^2/(aP) > T_{max} \Leftrightarrow Q > \sqrt{aPT_{max}/E} - b, \tag{7}$$

where T_{max} is $\max_i T_i$.

For all itineraries, we let $c_i = h_i$. Note that the objective of ISCA is to minimize the sum of movement-energy and loss-energy (see Eq. (5a)); since the shortest distance between r_i and each of the devices belonging to $\mathcal{V}_i$ is d, the overall loss-energy, i.e., $(\frac{(b+d)^2}{a} - 1)E \cdot m$, is fixed. The objective of ISCA is then reduced to minimizing the movement-energy.

Combining these, we get the following instance of ISCA. P and E could be of any reasonable value. $N = k$. $c_i = h_i$. T_i satisfies Eq. (6). $B_i = PT_i$. $M = m$. Q satisfies Eq. (7). d_{ij} satisfies Fig. 3. Does there exist a subset of $\mathcal{R}$, with cost no more than $(K - (\frac{(b+d)^2}{a} - 1)Em)$, that covers all devices?

It is not hard to see that the construction can be finished in polynomial time. Thus, we reduce solving the NP-complete SC problem to solving a special case of ISCA, implying that ISCA is NP-hard. It is easy to verify that ISCA is in NP. The theorem follows immediately.

We address three possible concerns. First, if T_i, t_{ij}, and f_{ij} are zeros in ISCA, is the ISCA problem exactly the SC problem? (and thus prove its hardness result.) The answer is no. We note that the sets and their elements are pre-determined in the SC problem, while in ISCA, the "belong to" relation is dynamic, i.e., a charging itinerary can cover any device if its charging capacity is not violated. Therefore, simply letting T_i, t_{ij}, and f_{ij} be zeros in ISCA would produce a trivial SC problem where each set (itinerary) contains all elements (devices), which is not NP-complete.

Second, it is not the first time a mobile charging problem is shown to be NP-complete. What are the differences between our proof and previous ones? The fundamental difference originates from the difference between our problem and previous ones. For example, Tong et al. [23] studied the problem of determining the locations and transmission powers of sensor nodes so as to minimize the total energy used by static chargers, and this problem is proven to be NP-complete by reducing the 3-CNF SAT problem to it; Shu et al. [26] investigated the problem of controlling velocities of multiple mobile chargers so as to maximize the network lifetime, and the problem is shown to be NP-complete by reducing the multi-objective shortest path problem to it; Chen et al. [31] studied the problem of maximizing the number of mobile devices that can be charged by a mobile charger within a given budget, and it is demonstrated to be NP-complete by reducing the Orienteering problem to it. And we focus on minimizing the amount of wasted energy by selecting charging itineraries and associations.

Third, the ISCA problem has its own unique characteristics; the values of f_{ij} and t_{ij} depend on the physical distance between a mobile charger and a device, and thus cannot be set arbitrarily. Therefore, ISCA with multipick admits constant approximations, but does not imply that the SC problem also admits constant approximations. That would be impossible unless P = NP. These unique features will play key roles in developing a constant approximation algorithm for ISCA with multipick.

3.5 Roadmap

In ISCA (Eq. (5)), each charging itinerary can be used once at most (Eq. (5i)). However, there may be more than one charger in the home station of each itinerary. Thus, we extend ISCA to the following general problem, ISCA-MP, where "MP" denotes multipick:[3]

$$\begin{aligned} \min \quad & \sum_{r_i \in \mathcal{R}} c_i y_i + \sum_{r_i \in \mathcal{R}} \sum_{s_j \in \mathcal{S}} f_{ij} x_{ij} \qquad \text{[ISCA-MP]} \\ \text{s.t.} \quad & \text{Eqs. (5e), (5f), (5g), and (5h)} \\ & y_i \in \mathcal{Z}^+, \qquad \forall r_i \in \mathcal{R} \end{aligned} \tag{8}$$

3. Note that constraints (5b), (5c), and (5d) are equations, and thus are omitted here.

Intuitively, ISCA-MP is harder to solve than ISCA. To help us gain some insights into the problem structure of ISCA-MP, we first study ISCA in Section 4, and we introduce a factor $O(\ln M)$ approximation algorithm and another simple yet practical heuristic algorithm. We then design a factor 10 approximation algorithm for ISCA-MP in Section 5.

4 Solution for ISCA

In this section, we present a factor $O(\ln M)$ approximation algorithm (Section 4.1) and a practical heuristic (Section 4.2).

Alg. GSA (Greedy Selection Algorithm)

1. $\mathcal{R}' \leftarrow \emptyset$; $\mathcal{S}' \leftarrow \emptyset$
2. $\forall i, j$, $x_{ij} \leftarrow 0$; $\forall i$, $y_i \leftarrow 0$
3. While $\mathcal{S} \setminus \mathcal{S}' \neq \emptyset$ do
4. If $\mathcal{R} \setminus \mathcal{R}' = \emptyset$, return failure
5. For each $r_i \in \mathcal{R} \setminus \mathcal{R}'$
6. Compute a subset $\mathcal{S}_i$ of $\mathcal{S} \setminus \mathcal{S}'$ by solving $(\max|\mathcal{S}_i|$, s.t. $\sum_{s_j \in \mathcal{S}_i} t_{ij} \leq T_i)$
7. $i' \leftarrow \arg\min_i \frac{c_i + \sum_{s_j \in \mathcal{S}_i} f_{ij}}{|\mathcal{S}_i|}$
8. $\mathcal{S}' \leftarrow \mathcal{S}' \cup \mathcal{S}_{i'}$, and $\forall j \in \mathcal{S}_{i'}$, $x_{i'j} \leftarrow 1$
9. $\mathcal{R}' \leftarrow \mathcal{R}' \cup \{i'\}$, and $y_{i'} \leftarrow 1$
10. Output x_{ij}s and y_is

4.1 Greedy Selection Algorithm

The greedy selection algorithm (GSA) is inspired by the reduction from SC to ISCA. The main idea of GSA is to *iteratively select the most cost-effective itinerary and remove the covered devices, until all devices are covered*. Here, when we say a device is "covered", we mean there is an itinerary that is responsible for charging it. "\" represents set minus. *Alg. GSA* shows the details.

$\mathcal{R}'$ denotes the set of itineraries that have already been selected, and $\mathcal{S}'$ denotes the set of devices that have already been covered. Initially, both of them are empty sets. In each iteration, we first compute the cost-effectiveness of all unselected itineraries and select the most cost-effective one. The cost-effectiveness can be computed as follows.

For each $r_i \in \mathcal{R} \setminus \mathcal{R}'$, we want to maximize the number of uncovered devices that it can cover. Therefore, we have the following trivial knapsack problem, where S_i is a subset of $\mathcal{S} \setminus \mathcal{S}'$:

$$\begin{aligned} \max \quad & |\mathcal{S}_i| \\ \text{s.t.} \quad & \sum_{s_j \in \mathcal{S}_i} t_{ij} \leq T_i. \end{aligned} \tag{9}$$

We would like to mention that Eq. (9) is a special case of the knapsack problem where the value of each item is 1. Therefore, greedily picking the device with the smallest t_{ij} is already optimal and costs only $O(M \log M)$ time. The cost-effectiveness of r_i is then defined as

$$\frac{c_i + \sum_{s_j \in \mathcal{S}_i} f_{ij}}{|\mathcal{S}_i|}.$$

We define the energy cost $ec(s_j)$ of s_j as the cost-effectiveness of the itinerary that covers s_j. Without loss of generality, we assume the order in which devices are covered is s_1, $s_2, \ldots, s_M$. Inspired by the performance guarantee analysis for the SC problem, we have the following theorem:

Theorem 2. *GSA is a factor $O(\ln M)$ approximation algorithm for ISCA.*

Proof. We denote by OPT the optimal solution for ISCA and consider the iteration in which s_j is covered by r_i. At the beginning of this iteration, $|\mathcal{S} \setminus \mathcal{S}'| > M - j + 1$; if we use the optimal solution to cover remaining devices, the total energy cost is at most OPT, implying that there exists an unselected itinerary having cost-effectiveness of at most $\frac{OPT}{|\mathcal{S} \setminus \mathcal{S}'|}$. We remember that GSA greedily selects the most cost-effective unselected itinerary, so we have

$$\begin{aligned} ec(s_j) &= \text{cost-effectiveness of } r_i \\ &\leq \frac{OPT}{|\mathcal{S} \setminus \mathcal{S}'|} \leq \frac{OPT}{M - j + 1}. \end{aligned}$$

It is obvious to see that the sum of movement-energy and loss-energy used in the solution obtained by GSA is $\sum_{s_j \in \mathcal{S}} ec(s_j)$. Since

$$\begin{aligned} \sum_{s_j \in \mathcal{S}} ec(s_j) &\leq \left(1 + \frac{1}{2} + \ldots + \frac{1}{M}\right) OPT \\ &\leq O(\ln M) OPT, \end{aligned}$$

the theorem follows immediately. □

GSA has at most N iterations. In each iteration, for each unselected itinerary, solving the (trivial) knapsack problem requires $O(M \log M)$ time, so the overall time complexity is $O(N^2 M \log M)$.

4.2 Modified GSA—A Practical Heuristic Algorithm

GSA has theoretic performance guarantee, but may perform poorly in practice. This section is devoted to improving GSA from the perspective of practice.

In each iteration of GSA, the most cost-effective itinerary is selected regardless of the other itineraries, devices, and their interrelationships. This is the key observation that helps us improve GSA. The Modified GSA is shown in *Alg. MGSA*. The difference compared with GSA is marked in blue (lines 6-9).The main idea of MGSA is as follows.

In each iteration, instead of selecting the most cost-effective itinerary, *MGSA selects the itinerary that costs a minimal energy to cover the devices that may take up more energy if they are otherwise covered by one of the other unselected itineraries*. This intuition is captured by variable g_{ij}: for each $r_i \in \mathcal{R} \setminus \mathcal{R}'$ and each $s_j \in \mathcal{S} \setminus \mathcal{S}'$, g_{ij} is defined as the average cost of s_j if it is covered by the itineraries in $\mathcal{R} \setminus (\mathcal{R}' \cup \{i\})$, i.e.,

$$g_{ij} = \frac{1}{|\mathcal{R} \setminus (\mathcal{R}' \cup \{i\})|} \sum_{r_k \in \mathcal{R} \setminus (\mathcal{R}' \cup \{i\})} f_{kj}.$$

Then, for each $r_i \in \mathcal{R} \setminus \mathcal{R}'$, we try to find a subset $\mathcal{S}_i$ of uncovered devices that maximize $\sum_{s_j \in \mathcal{S}_i} g_{ij}$. Thus, we have the following knapsack problem:

$$\begin{aligned} \max \quad & \sum_{s_j \in \mathcal{S}_i} g_{ij} \\ \text{s.t.} \quad & \sum_{s_j \in \mathcal{S}_i} t_{ij} \le T_i. \end{aligned} \tag{10}$$

We then select the itinerary that minimizes the energy cost, i.e., $c_i + \sum_{s_j \in \mathcal{S}_i} f_{ij}$, and make some updates. Solving Eq. (10) through dynamic programming costs $O(MT_i)$ time. Thus, the overall complexity of MGSA is $O(N^2 M T_{max})$.

Alg. MGSA (Modified Greedy Selection Algorithm)

1. $\mathcal{R}' \leftarrow \emptyset$; $\mathcal{S}' \leftarrow \emptyset$
2. $\forall i, j, x_{ij} \leftarrow 0$; $\forall i, y_i \leftarrow 0$
3. While $\mathcal{S} \setminus \mathcal{S}' \neq \emptyset$ do
4. If $\mathcal{R} \setminus \mathcal{R}' = \emptyset$, return failure
5. For each $r_i \in \mathcal{R} \setminus \mathcal{R}'$
6. For each $s_j \in \mathcal{S} \setminus \mathcal{S}'$
7. $g_{ij} \leftarrow \frac{1}{|\mathcal{R} \setminus (\mathcal{R}' \cup \{i\})|} \sum_{r_k \in \mathcal{R} \setminus (\mathcal{R}' \cup \{i\})} f_{kj}$
8. Compute a subset $\mathcal{S}_i$ of $\mathcal{S} \setminus \mathcal{S}'$ by solving $(\max \sum_{s_j \in \mathcal{S}_i} g_{ij}$, s.t. $\sum_{s_j \in \mathcal{S}_i} t_{ij} \le T_i)$
9. $i' \leftarrow \arg\min_{\mathcal{S}_i \neq \emptyset} (c_i + \sum_{s_j \in \mathcal{S}_i} f_{ij})$
10. $\mathcal{S}' \leftarrow \mathcal{S}' \cup \mathcal{S}_{i'}$, and $\forall j \in \mathcal{S}_{i'}, x_{i'j} \leftarrow 1$
11. $\mathcal{R}' \leftarrow \mathcal{R}' \cup \{i'\}$, and $y_{i'} \leftarrow 1$
12. Output x_{ij}s and y_is

4.3 Summary

In each iteration of MGSA, we think ahead by selecting an itinerary that, on average, consumes less loss-energy than the remaining itineraries to cover a subset of uncovered devices. Though we cannot provide any theoretical performance guarantee for MGSA at this stage, it works better than GSA in the evaluations presented in Section 7.

5 Solution for ISCA-MP

In this section, we examine ISCA in a general setting by *allowing an itinerary to be selected multiple times*, i.e., ISCA-MP. We first give the relaxed primal and dual problems of ISCA-MP (Section 5.1) and explain their slackness conditions (Section 5.2); then, we present the transformation (Section 5.3) and a constant-factor approximation algorithm (Section 5.4). Finally, we show how to revert to the original problem, i.e., ISCA-MP (Section 5.5). We also provide a concrete example that may help illustrate the details (Section 5.6).

5.1 Primal and Dual Problems

The LP-relaxation of ISCA-MP can be obtained by letting $0 \le x_{ij} \le 1$ and $0 \le y_i \le 1$. Since ISCA-MP is a minimization problem, (≤ 1)s are redundant and thus, are discarded. The solution to this fractional CSRA-MP is a lower bound of ISCA-MP. In fact, the solution to ISCA-MP also provides a lower bound of ISCA

$$\begin{aligned} \min \quad & \sum_{r_i \in \mathcal{R}} c_i y_i + \sum_{r_i \in \mathcal{R}} \sum_{s_j \in \mathcal{S}} f_{ij} x_{ij} \qquad \text{[ISCA-MP-PL]} \\ \text{s.t.} \quad & \text{Eqs. (5e), (5f), and (5g)} \\ & x_{ij} \ge 0, \qquad \forall s_j \in \mathcal{S}, r_i \in \mathcal{R} \\ & y_i \ge 0, \qquad \forall r_i \in \mathcal{R}. \end{aligned} \tag{11}$$

In the above formulation, "PL" refers to "primal". Introducing variables αs, βs, and θs corresponding to Eqs. (5e), (5f), and (5g), respectively, we have the following dual problem, where "DL" refers to "dual":

$$\max \quad \sum_{s_j \in \mathcal{S}} \alpha_j \qquad \text{[ISCA-MP-DL]} \tag{12a}$$

$$\text{s.t.} \quad T_i \theta_i + \sum_{s_j \in \mathcal{S}} \beta_{ij} \le c_i, \quad \forall r_i \in \mathcal{R} \tag{12b}$$

$$\alpha_j - \beta_{ij} - t_{ij} \theta_i \le f_{ij}, \quad \forall s_j \in \mathcal{S}, r_i \in \mathcal{R} \tag{12c}$$

$$\alpha_j \ge 0, \quad \forall s_j \in \mathcal{S} \tag{12d}$$

$$\beta_{ij} \ge 0, \quad \forall s_j \in \mathcal{S}, r_i \in \mathcal{R} \tag{12e}$$

$$\theta_i \ge 0, \quad \forall r_i \in \mathcal{R} \tag{12f}$$

According to the weak duality theorem [33], the dual problem, i.e., ISCA-MP-DL gives a lower bound on the optimal value of the primal problem, i.e., ISCA-MP-PL. We will see shortly in Section 5.4 that this lower bound will be very useful in obtaining the approximation ratio.

5.2 Understanding Dual Variables

In this section, we use the complementary slackness conditions [33] to help readers better understand the dual problem, i.e., ISCA-MP-DL.

The primal complementary slackness conditions are as follows:

$$\text{(a) } y_i > 0 \Rightarrow T_i \theta_i + \sum_{s_j \in \mathcal{S}} \beta_{ij} = c_j, \quad \forall r_i \in \mathcal{R};$$

$$\text{(b) } x_{ij} > 0 \Rightarrow \alpha_j - \beta_{ij} - t_{ij} \theta_i = f_{ij}, \quad \forall s_j \in \mathcal{S}, r_i \in \mathcal{R}.$$

The dual complementary slackness conditions are as follows:

$$\text{(c) } \alpha_j > 0 \Rightarrow \sum_{r_i \in \mathcal{R}} x_{ij} = 1, \quad \forall s_j \in \mathcal{S};$$

$$\text{(d) } \beta_{ij} > 0 \Rightarrow y_i - x_{ij} = 0, \quad \forall s_j \in \mathcal{S}, r_i \in \mathcal{R};$$

$$\text{(e) } \theta_i > 0 \Rightarrow T_i y_i - \sum_{s_j \in \mathcal{S}} t_{ij} x_{ij} = 0, \quad \forall r_i \in \mathcal{R}.$$

By condition (a), if an itinerary is selected, then $T_i \theta_i + \sum_{s_j \in \mathcal{S}} \beta_{ij} = c_j$. By condition (d), we suppose $y_i = 1$. If $x_{ij} = 1$, then $\beta_{ij} > 0$; otherwise, $\beta_{ij} = 0$. By condition (b), if $x_{ij} = 1$, then $\alpha_j - \beta_{ij} - t_{ij} \theta_i = f_{ij}$.

Combining the conditions, we can take α_j *as the total price paid by device* s_j *for the charging service, and* α_j *can be partitioned into three parts*: β_{ij}, $t_{ij}\theta_i$, and f_{ij}. The first two parts pay for the movement-energy cost of r_i (by condition (a)); if we take θ_i as the unit price of charging time, then, β_{ij} is a fixed part, and $t_{ij}\theta_i$ is a dynamic part depending on t_{ij}. The last part of α_j is f_{ij}, which pays for loss-energy when s_j is being charged.

5.3 Transformation

There are three types of variables, α, β, and θ, in the ISCA-MP-DL problem. We want to eliminate one of them (say, θ) and transform ISCA-MP-PL and ISCA-MP-DL into a new pair of primal and dual programs that have only two

variables. We want to solve them, and finally to revert to the original integral problem.

Let $\theta_i = \frac{9c_i}{10T_i}$. ISCA-MP-DL becomes

$$\max \quad \sum_{s_j \in \mathcal{S}} \alpha_j \qquad \text{[ISCA-MP-DL-T]} \tag{13a}$$

$$\text{s.t.} \sum_{s_j \in \mathcal{S}} \beta_{ij} \leq \frac{c_i}{10}, \qquad \forall r_i \in \mathcal{R} \tag{13b}$$

$$\alpha_j - \beta_{ij} \leq f_{ij} + \frac{9c_i t_{ij}}{10T_i}, \qquad \forall s_j \in \mathcal{S}, r_i \in \mathcal{R} \tag{13c}$$

$$\alpha_j \geq 0, \qquad \forall s_j \in \mathcal{S} \tag{13d}$$

$$\beta_{ij} \geq 0, \qquad \forall s_j \in \mathcal{S}, r_i \in \mathcal{R} \tag{13e}$$

The integral dual of ISCA-MP-DL-T, i.e., the transformed ISCA-MP, is as follows:

$$\begin{aligned} \min \quad & \sum_{r_i \in \mathcal{R}} \frac{c_i y_i}{10} + \sum_{r_i \in \mathcal{R}} \sum_{s_j \in \mathcal{S}} \left(f_{ij} + \frac{9c_i t_{ij}}{10T_i} \right) x_{ij} \text{[ISCA-MP-T]} \\ \text{s.t.} \quad & \text{Eqs. (5e), (5f), and (5h)} \\ & y_i \in \mathcal{Z}^+, \qquad \forall r_i \in \mathcal{R} \end{aligned} \tag{14}$$

Note that the constraint Eq. (5g) is discarded in Eq. (14); therefore, in ISCA-MP-T, there is no constraint on the capacity of each itinerary.

5.4 Approximation Algorithm for ISCA-MP-T

We now consider two problems: the primal problem, i.e., ISCA-MP-T, and the dual problem, i.e., ISCA-MP-DL-T. There is a factor three approximation algorithm for the facility location problem in [33]. Based on that algorithm and some special properties of ISCA-MP-T, we now propose a factor nine approximation algorithm for ISCA-MP-T using the primal-dual schema, shown in Alg. PDA. The main intuition behind PDA is as follows.

Alg. PDA (Primal-Dual Schema-Based Algorithm)

Part I: **Compute dual solution**

1. $\forall i$, $tselected_i \leftarrow 0$
2. $\forall j$, $\alpha_j \leftarrow 0$, $covered_j \leftarrow 0$, $chost_j \leftarrow 0$
3. $\forall i, j$, $\beta_{ij} \leftarrow 0$, $full_{ij} \leftarrow 0$, $positive_{ij} \leftarrow 0$
4. Timestamp $ts \leftarrow 0$
5. While there is any uncovered device do
6. $\quad ts \leftarrow ts + 1$
7. $\quad$ For each s_j that satisfies $covered_j = 0$ do
8. $\quad\quad \alpha_j \leftarrow \alpha_j + 1$
9. $\quad\quad$ For each r_i that satisfies $\alpha_j = f_{ij} + \frac{9c_i t_{ij}}{10T_i}$ do
10. $\quad\quad\quad full_{ij} \leftarrow 1$
11. $\quad\quad\quad$ If $tselected_i = 1$ and $covered_j = 0$ do
12. $\quad\quad\quad\quad covered_j \leftarrow 1$, $chost_j \leftarrow r_i$
13. $\quad\quad$ For each r_i that satisfies $\alpha_j > f_{ij} + \frac{9c_i t_{ij}}{10T_i}$ do
14. $\quad\quad\quad \beta_{ij} \leftarrow \beta_{ij} + 1$, $positive_{ij} \leftarrow 1$
15. $\quad\quad\quad$ If $\sum_{s_j \in \mathcal{S}} \beta_{ij} = \frac{c_i}{10}$ do
16. $\quad\quad\quad\quad tselected_i \leftarrow 1$
17. $\quad\quad\quad\quad$ For each s_k that satisfies $covered_k = 0$ and $full_{ik} = 1$ do
18. $\quad\quad\quad\quad\quad covered_k \leftarrow 1$, $chost_k \leftarrow r_i$
19. αs and βs form a dual solution to ISCA-MP-DL-T

PDA starts with a primal infeasible solution and a dual feasible solution. It iteratively improves the feasibility of the primal solution and the optimality of the dual solution. It ensures that (i) the primal solution is always extended integrally, and that (ii) the value of the dual solution is at least f times as large as the value of the primal solution. Since the dual solution is a lower bound on the optimal value of the primal solution, the approximation ratio is then equal to f.

Alg. PDA (Primal-Dual schema-Based Algorithm)

Part II: **Compute integral primal solution**

21. $\forall i, j$, $x_{ij} \leftarrow 0$; $\forall i$, $y_i \leftarrow 0$, $fselected_i \leftarrow 0$
22. $\mathcal{R}_{ts} \leftarrow \{r_i | tselected_i = 1\}$
23. Construct a graph G with $\mathcal{R}_{ts}$ as vertex set. For each pair of $r_i, r_k \in \mathcal{R}_{ts}$, there is an edge between them if and only if $\exists s_j \in \mathcal{S}$, s.t. $positive_{ij} = positive_{kj} = 1$.
24. Find a maximal independent vertex set in G with non-decreasing order of $\frac{c_i}{T_i}$, say $\mathcal{D}$.
25. For each $r_i \in \mathcal{D}$, set $y_i \leftarrow 1$, $fselected_i \leftarrow 1$.
26. For each s_j do
27. $\quad \mathcal{R}_j \leftarrow \{r_i | r_i \in \mathcal{R}_{ts}, \beta_{ij} > 0\}$
28. $\quad$ If $\mathcal{R}_j \cap \mathcal{D} \neq \emptyset$, then $\mathcal{R}_j \cap \mathcal{D}$ has only one element r_i.
29. $\quad\quad$ Set $x_{ij} \leftarrow 1$, s_j is called closely covered.
30. $\quad$ Else if $chost_j \in \mathcal{D}$, let $r_k \leftarrow chost_j$
31. $\quad\quad$ Set $x_{kj} \leftarrow 1$, s_j is called normally covered.
32. $\quad$ Otherwise, $\mathcal{D}$ must contain r_h, such that r_k and r_h are neighbors in G, and $c_h/T_h \leq c_k/T_k$
33. $\quad\quad$ Set $x_{hj} \leftarrow 1$, s_j is called loosely covered.
34. xs and ys form an integral solution to ISCA-MP-T

PDA consists of two parts, which correspond to computing dual and integral primal solutions, respectively. In the following, we first introduce these two parts and then provide the analysis of the approximation ratio.

5.4.1 Compute Dual Solution

The objective of ISCA-MP-DL-T is to maximize $\sum_{s_j \in \mathcal{S}} \alpha_j$. The first part of PDA tries to increase αs as much as possible and maintains Eqs. (13b) and (13c).

All events are associated with a timestamp ts. When ts is zero, each itinerary is not temporarily selected ($tselected$); each α is 0; each device is not covered ($covered$); the covering host ($chost$) of each device is 0; each β is 0; the connection between r_i and s_j is neither *full* nor *positive*.

PDA raises α by one for each uncovered device as ts grows by one (line 8). For each r_i that satisfies $\alpha_j = f_{ij} + \frac{9c_i t_{ij}}{10T_i}$, PDA runs as follows:

- the connection between itinerary r_i and device s_j becomes *full* (line 10);
- if r_i is temporarily selected and s_j is not covered, we change s_j into covered and its covering host is r_i (lines 11-12).

And for each r_i that satisfies $\alpha_j > f_{ij} + \frac{9c_i t_{ij}}{10T_i}$, PDA runs as follows:

- β_{ij} is increased by one and the corresponding connection is set to be positive (line 14), ensuring that Eq. (13 c) is not violated;
- if $\sum_{s_j \in \mathcal{S}} \beta_{ij} = \frac{c_i}{10}$, then r_i is marked as temporarily selected, all uncovered devices that have full

connections to r_i are declared covered, and r_i is the covering host for each of them.

When all devices become covered, the first half of PDA terminates.

5.4.2 Compute Integral Primal Solution

The second part of PDA computes an integral solution to ISCA-MP-T. In fact, the αs and βs obtained from the first half of PDA give us some clues for finding an integral solution to ISCA-MP-T.

Initially, each x_{ij} is 0; each y_i is 0; each itinerary is not finally selected ($fselected$). $\mathcal{R}_{ts}$ is the set of temporarily selected itineraries. In fact, $\mathcal{R}_{ts}$ contains some unnecessary itineraries. In lines 23-25, we select a subset of $\mathcal{R}_{ts}$ as the finally selected itineraries. We first construct a graph G with $\mathcal{R}_{ts}$ as vertex set. For each pair of $r_i, r_k \in \mathcal{R}_{ts}$, there is an edge between them if and only if $\exists s_j \in \mathcal{S}$, s.t. $positive_{ij} = positive_{kj} = 1$. Then we find a maximal independent vertex set in G, say $\mathcal{D}$, as the set of finally selected itineraries. $\mathcal{D}$ is obtained as follows: we sort the vertex set of G in non-decreasing order of $\frac{c_i}{T_i}$ and then check whether each vertex (i.e., itinerary) can be added into the maximal set. The itinerary selection part is done. The rest of the task is itinerary association.

For each s_j, we denote $\mathcal{R}_j$ as the set of temporarily selected itineraries that have positive connections to s_j (line 27). There are three cases:

- If $\mathcal{R}_j \cap \mathcal{D} \neq \emptyset$, since $\mathcal{D}$ is a maximal independent vertex set on G, $\mathcal{R}_j \cap \mathcal{D}$ has only one element, say r_i; thus we set $x_{ij} \leftarrow 1$, and s_j is called *closely covered*;
- Otherwise, the covering host of s_j, say r_k, is in $\mathcal{D}$. We set $x_{kj} \leftarrow 1$, and s_j is called *normally covered*;
- In the remaining case, $\mathcal{D}$ must contain r_h such that r_k and r_h are neighbors in G, and $c_h/T_h \leq c_k/T_k$ (because $\mathcal{D}$ is a maximal independent set, again); we then set $x_{hj} \leftarrow 1$, and s_j is called *loosely covered*.

5.4.3 Dual Feasibility

We have to check whether the obtained αs and βs satisfy the four constraints in Eq. (13). Constraints (13(e)) and (13(d)) are trivial. In lines 13-14, whenever α_j is larger than $f_{ij} + \frac{9c_i t_{ij}}{10T_i}$, we also increase β_{ij} by one, making sure constraint (13(c)) is not violated. In lines 15-18, whenever $\sum_{s_j \in \mathcal{S}} \beta_{ij} = \frac{c_i}{10}$, all uncovered devices that have full connections to r_i will be marked as covered, implying that those β_{ij}s will not increase any more.

5.4.4 Primal Feasibility

We check whether the obtained xs and ys violate the four constraints in Eq. (14). For Eq. (5 e), lines 26-33 of PDA guarantee that each s_j is charged by one of the finally selected itineraries. For Eq. (5f), lines 26-33 guarantee that devices can only be charged by the finally-selected itineraries. The rest is trivial.

5.4.5 Approximation Ratio Analysis

We denote by OPT the optimal solution to ISCA-MP-T. Due to the weak duality theorem [33], $\sum_{s_j \in \mathcal{S}} \alpha_j$ is a lower bound of OPT. We now try to find a upper bound of

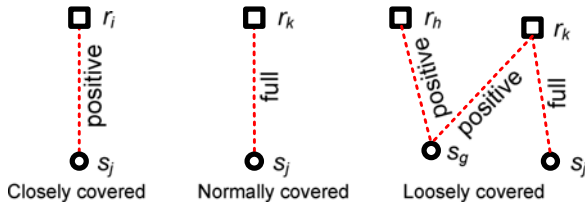

Fig. 4. Three types of *being covered* (See lines 26-33 of Alg. PDA). Note that a positive connection is also full, but a full connection may be not positive.

$$\sum_{r_i \in \mathcal{R}} \frac{c_i y_i}{10} + \sum_{r_i \in \mathcal{R}} \sum_{s_j \in \mathcal{S}} \left(f_{ij} + \frac{9c_i t_{ij}}{10T_i} \right) x_{ij},$$

in terms of $\sum_{s_j \in \mathcal{S}} \alpha_j$.

According to Alg. PDA, each device is covered by one of the three types (see lines 26-33): closely covered (*ccovered*), normally covered (*ncovered*), and loosely covered (*lcovered*). Fig. 4 gives an illustration, where squares represent itineraries.

For each *ccovered* device s_j, we suppose that r_i covers it in the final solution. Since the connection between r_i and s_j is positive, α_j can be split into two parts: β_{ij}, and $(f_{ij} + 9c_i t_{ij}/(10T_i))$ (lines 9, and 13-14). It is trivial to see that

$$\sum_{s_j \text{ is ccovered, and } r_i \in \mathcal{D}} \beta_{ij} = \sum_{r_i \in \mathcal{R}} \frac{c_i y_i}{10}, \tag{15}$$

and the second part of α_j pays for the connection cost,

$$\sum_{s_j \text{ is ccovered, and } r_i \in \mathcal{D}} \alpha_j - \beta_{ij} = \sum_{r_i \in \mathcal{R}} \sum_{s_j \text{ is ccovered}} \left(f_{ij} + \frac{9c_i t_{ij}}{10T_i} \right) x_{ij}. \tag{16}$$

For each *ncovered* device s_j, we suppose that r_k covers it in the final solution. Since the connection between r_k and s_j is full, α_j pays for the connection cost,

$$\sum_{s_j \text{ is ncovered, and } r_i \in \mathcal{D}} \alpha_j = \sum_{r_i \in \mathcal{R}} \sum_{s_j \text{ is ncovered}} \left(f_{ij} + \frac{9c_i t_{ij}}{10T_i} \right) x_{ij}. \tag{17}$$

For *lcovered* devices, we have the following theorem:

Theorem 3. *For lcovered devices, we have*

$$\sum_{s_j \text{ is lcovered, and } r_i \in \mathcal{D}} 9\alpha_j \geq \sum_{r_i \in \mathcal{R}} \sum_{s_j \text{ is lcovered}} \left(f_{ij} + \frac{9c_i t_{ij}}{10T_i} \right) x_{ij}. \tag{18}$$

Proof. For each lcovered device s_j, we suppose that r_h covers it in the final solution and that r_k is its covering host (see Fig. 4). According to line 23 of Alg. PDA, there must exist another s_g that has positive connections with both r_k and r_h. It is trivial to see that

$$\begin{aligned} \alpha_j &\geq f_{kj} + 9c_k t_{kj}/(10T_k), \\ \alpha_g &\geq f_{kg} + 9c_k t_{kg}/(10T_k), \\ \alpha_g &\geq f_{hg} + 9c_h t_{hg}/(10T_h). \end{aligned}$$

We denote by ts_h and ts_k the timestamps when r_h and r_k are marked as temporarily selected (line 16), respectively. Since r_k is the covering host of s_j, we have $\alpha_j \geq ts_k$. Since the connection between s_g and either r_h or r_k is positive, we have $\alpha_g \geq \min(ts_h, ts_k)$. Therefore, $\alpha_j \geq \alpha_g$.

According to lines 24 and 32-33, we have $c_h/T_h \leq c_k/T_k$. To prove Eq. (18), it is sufficient to prove that

$$
\begin{aligned}
& f_{hj} + \frac{9c_h t_{hj}}{10T_h} \\
&= \frac{E}{a}\left[(b+d_{hj})^2 - a\right] + \frac{9Ec_h(b+d_{hj})^2}{10aPT_h} \quad \text{(Eqs. (3) and (4))} \\
&\leq \frac{E}{a}\left[(b+d_{hg}+d_{kg}+d_{kj})^2 - a\right] \\
&\quad + \frac{9c_h E(b+d_{hg}+d_{kg}+d_{kj})^2}{10aPT_h} \quad \text{(triangle inequality)} \\
&\leq \frac{3E}{a}\left[(b+d_{hg})^2 + (b+d_{kg})^2 + (b+d_{kj})^2 - 3a - (8b^2-2a)\right] \\
&\quad + \frac{27c_h E[(b+d_{hg})^2 + (b+d_{kg})^2 + (b+d_{kj})^2]}{10aPT_h} \\
&\leq \frac{3E}{a}\left[(b+d_{hg})^2 - a + (b+d_{kg})^2 - a + (b+d_{kj})^2 - a\right] \\
&\quad + \left[\frac{27c_h E(b+d_{hg})^2}{10aPT_h} + \frac{27c_h E(b+d_{kg})^2}{10aPT_h} + \frac{27c_h E(b+d_{kj})^2}{10aPT_h}\right] \\
&\leq 3(f_{hg}+f_{kg}+f_{kj}) + 3\left(\frac{9c_h t_{hg}}{10T_h} + \frac{9c_h t_{kg}}{10T_h} + \frac{9c_h t_{kj}}{10T_h}\right) \\
&\leq 3(f_{hg}+f_{kg}+f_{kj}) + 3\left(\frac{9c_h t_{hg}}{10T_h} + \frac{9c_k t_{kg}}{10T_k} + \frac{9c_k t_{kj}}{10T_k}\right) \\
&\leq 3(\alpha_g + \alpha_g + \alpha_j) \\
&\leq 9\alpha_j,
\end{aligned}
$$

where the third "$\leq$" is due to $8b^2 \geq 2a$, as a and b are know constants, and b is much bigger than a. □

Combining the above analyses and Theorem 3, we have

Theorem 4. *PDA is a factor nine approximation algorithm for ISCA-MP-T.*

Proof. As previously mentioned, due to the weak duality theorem, $\sum_{s_j \in \mathcal{S}} \alpha_j$ is a lower bound of OPT. Eqs. (15), (16), (17), and (18), help us build a upper bound of $\sum_{r_i \in \mathcal{R}} \frac{c_i y_i}{10} + \sum_{r_i \in \mathcal{R}} \sum_{s_j \in \mathcal{S}} (f_{ij} + \frac{9c_i t_{ij}}{10T_i}) x_{ij}$ in terms of $\sum_{s_j \in \mathcal{S}} \alpha_j$, i.e.,

$$
\begin{aligned}
& \sum_{r_i \in \mathcal{R}} \frac{c_i y_i}{10} + \sum_{r_i \in \mathcal{R}} \sum_{s_j \in \mathcal{S}} \left(f_{ij} + \frac{9c_i t_{ij}}{10T_i}\right) x_{ij} \\
&\leq 9 \sum_{r_i \in \mathcal{R}} \frac{c_i y_i}{10} + \sum_{r_i \in \mathcal{R}} \sum_{s_j \in \mathcal{S}} \left(f_{ij} + \frac{9c_i t_{ij}}{10T_i}\right) x_{ij} \qquad (19) \\
&\leq 9 \sum_{s_j \in \mathcal{S}} \alpha_j \\
&\leq 9 \cdot OPT,
\end{aligned}
$$

the theorem follows immediately. □

5.5 Retransformation: Revert to ISCA-MP

In the previous sections, we have developed an approximation algorithm of factor 9 for ISCA-MP-T. We now show how to modify the results obtained by PDA for ISCA-MP.

We denote by x's and y's the solution to ISCA-MP, and by xs and ys the solution generated by PDA for ISCA-MP-T. In order to respect constraint (5g), we let

$$
x'_{ij} = x_{ij}, \text{ and } y'_i = \left\lceil \frac{\sum_{s_j \in \mathcal{S}} t_{ij} x_{ij}}{T_i} \right\rceil. \qquad (20)
$$

	r_1	r_2	r_3	r_4
c	10	20	20	40
T	3	6	9	12

t_{ij}	s_1	s_2	s_3	s_4
r_1	1	1	4/3	2
r_2	4/3	1	2	1
r_3	1/2	2	3	1
r_4	1	2	4/3	1

f_{ij}	s_1	s_2	s_3	s_4
r_1	2	2	3	4
r_2	3	2	4	2
r_3	1	3	4	2
r_4	2	4	3	2

$f_i + \frac{9c_i t_{ij}}{10T_i}$	s_1	s_2	s_3	s_4
r_1	5	5	7	10
r_2	7	5	10	5
r_3	2	9	10	4
r_4	5	10	7	5

(a) PDA inputs

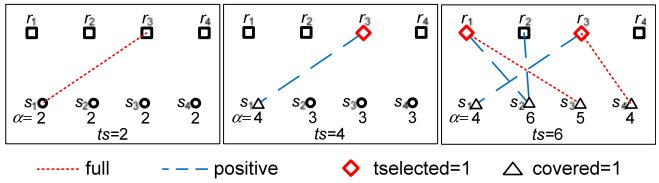

(b) PDA in different timestamps

Fig. 5. Example of running PDA. Note that the α of a device will not increase after being covered. The final solution is, s_1 and s_2 are closely covered by r_3 and r_1, respectively; s_3 and s_4 are normally covered by r_1 and r_3, respectively.

Theorem 5. *PDA plus Eq. (20) is a factor 10 approximation algorithm for ISCA with multipick.*

Proof. Notice that $y'_i \leq y_i + \frac{\sum_{s_j \in \mathcal{S}} t_{ij} x_{ij}}{T_i}$, then we have

$$
\begin{aligned}
& \sum_{r_i \in \mathcal{R}} c_i y'_i + \sum_{r_i \in \mathcal{R}} \sum_{s_j \in \mathcal{S}} f_{ij} x'_{ij} \\
&\leq \sum_{r_i \in \mathcal{R}} c_i y'_i + \frac{10}{9} \sum_{r_i \in \mathcal{R}} \sum_{s_j \in \mathcal{S}} f_{ij} x'_{ij} \\
&\leq \frac{10}{9}\left[\frac{9}{10} \sum_{r_i \in \mathcal{R}} c_i \left(y_i + \frac{\sum_{s_j \in \mathcal{S}} t_{ij} x_{ij}}{T_i}\right) + \sum_{r_i \in \mathcal{R}} \sum_{s_j \in \mathcal{S}} f_{ij} x'_{ij}\right] \\
&= \frac{10}{9}\left[9 \sum_{r_i \in \mathcal{R}} \frac{c_i y_i}{10} + \sum_{r_i \in \mathcal{R}} \sum_{s_j \in \mathcal{S}} \left(f_{ij} + \frac{9c_i t_{ij}}{10T_i}\right) x_{ij}\right] \\
&\leq \frac{10}{9} 9 \sum_{s_j \in \mathcal{S}} \alpha_j \\
&\leq 10 \sum_{s_j \in \mathcal{S}} \alpha_j \\
&\leq 10 \cdot OPT,
\end{aligned}
$$

the theorem follows immediately. □

Hereto, we have a constant-factor approximation for ISCA-MP, i.e., charging with fixed itineraries in a general setting.

Let $L = \max_{i,j}(c_i/10 + f_{ij} + 9c_i t_{ij}/(10T_i))$. In the first part of PDA, the maximal timestamp is at most L; in each iteration, PDA scans every connection between itineraries and uncovered devices. In the second part, constructing G requires $O(MN)$ time; finding a maximal independent vertex set needs $O(N^2 \log N)$ time. Therefore, the worst-case time complexity of PDA is $O(LMN + N^2 \log N)$.

5.6 Example of Running PDA

We use an example to better illustrate the details of PDA.

Fig. 5a shows the inputs (i.e., c_is, T_is, t_{ij}s, and f_{ij}s) of the algorithm. There are 4 itineraries and 4 devices to cover. Fig. 5b shows how PDA works in different timestamps.

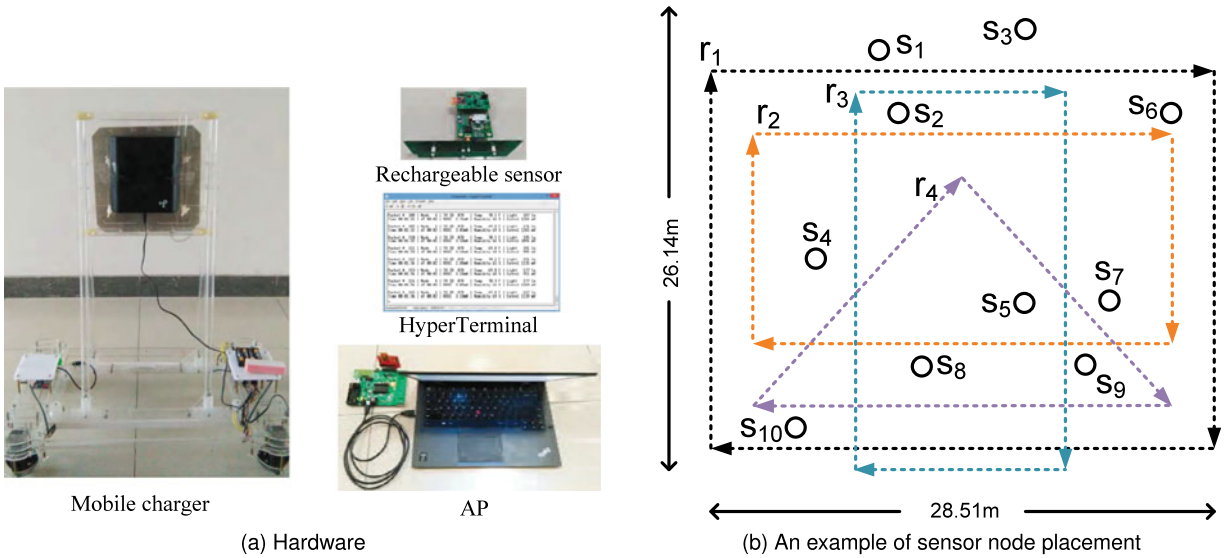

Fig. 6. Our testbed consists of 4 TX91501 power transmitters produced by Powercast [34], 10 rechargeable sensor nodes, and an AP.

In the first part of PDA, when $ts = 2$, since $\alpha_1 = 2 = f_{31} + 9c_3t_{31}/(10T_3)$, the connection between r_3 and s_1 becomes full. When $ts = 4$, since $\sum_{s_j} \beta_{3j} = \beta_{31} = 2 = c_3/10$, r_3 becomes temporarily selected, and all devices (here, only s_1) that have full connections with r_3 are declared as being covered. Later, when α_4 changes to 4, the connection between s_4 and r_3 becomes full, that is, s_4 is covered and its covering host is r_3. α_1 and α_4 will not increase any more hereafter. When $ts = 6$, it is not hard to verify that r_1 is temporarily selected and covers s_2 and s_3.

In the second part of PDA, $\mathcal{R}_{ts} = \{r_1, r_3\}$. Since there is not any device that has positive connections with both of them, the maximal independent set $\mathcal{D}$ is $\{r_1, r_3\}$, too. In the final solution, s_1 and s_2 are closely covered by r_3 and r_1, respectively; s_3 and s_4 are normally covered by r_1 and r_3, respectively. The energy cost of this solution is 38 (see Eq. (5 a)), while the optimal solution is to select r_1 twice, yielding a cost of 31. Note that though the approximation factor of PDA is 10, on average, it works much better than the bound.

5.7 Summary

We present PDA for ISCA-MP in this section. We first relax integral variables to get ISCA-MP-PL and its dual ISCA-MP-DL. We then fix one variable in ISCA-MP-DL to get ISCA-MP-DL-T and its corresponding transformed primal integral problem ISCA-MP-T. We design an algorithm, PDA, for ISCA-MP-T with an approximation ratio of 9. Finally we re-transform ISCA-MP-T to ISCA-MP and prove that PDA is a factor 10 approximation algorithm for ISCA-MP.

6 Field Experiments

To better validate the proposed algorithms, we conduct real field experiments in this section.

6.1 Experimental Setup

We develop a testbed that consists of 4 TX91501 power transmitters produced by Powercast [34], 10 rechargeable sensor nodes , and an AP, as shown in Fig. 6. All devices are deployed within a square of 26.14 $\times$ 28.51 m. Rechargeable sensor nodes are randomly placed within this area. We assume that the amount of energy required by each sensor node is 10 mJ.

The transmitting power of TX91501 is 3 W. We combine a TX91501 with a mobile robot to obtain a mobile charger. The movement of the charger is supported by the battery and a charger consumes roughly 4J per meter. The battery capacity of each transmitter is 1,300 J. We choose four candidate itineraries, as shown in Fig. 6. The physical lengths of these itineraries are 99.79, 71.28, 66.52, and 59.09 m, respectively. The charging area of a TX91501 transmitter is roughly a sector with with an angle of 60°, therefore, when a mobile charger approaches a sensor node, we may need to manually adjust the orientation of the TX91501 transmitter to make sure that the sensor node to be charged is within the charging area of the charger.

In our testbed, the AP connecting to a laptop is responsible for collecting the received power information (along with temperature, light, and humidity information) of each rechargeable sensor node and sending it the HyperTerminal on the laptop, as shown in Fig. 6.

6.2 Experimental Results

We are interested in comparing four algorithms, including OPT, PDA, GSA, and RAN. We use the optimal *fractional* solution by solving the LP-relaxation of Eqs. (5) and (8) using the Python PuLP package [35] to replace the optimal integral solution OPT, as the former is a lower bound of the latter. The random solution RAN is obtained by first randomly selecting itineraries and then randomly determining charging association, under the capacity constraints. We fix four candidate itineraries and run four algorithms on ten different placements of rechargeable sensor nodes. The average, maximum, and minimum results among the ten runs are shown in Figs. 7, 9, and 10.

Fig. 7 shows the comparison results. Generally speaking, PDA performs better than GSA, and GSA outperforms RAN. PDA allows each itinerary to be selected more than once, thus, there are more opportunities for PDA to improve the results than GSA. The gap between PDA and OPT is at most 23 percent of OPT, which is consistent with our theoretic analysis. When rechargeable sensor nodes are placed

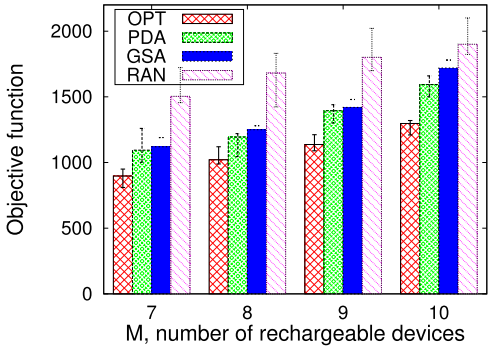

Fig. 7. Comparison results of four algorithms in field experiments.

as shown in Fig. 6b, we also plot the charging time (i.e., t_{ij}) of each sensor node with OPT and PDA in Fig. 8. With OPT, itineraries r_1 and r_4 are chosen: r_1 is responsible for charging s_1, s_2, s_3, s_6, and s_{10}, while r_4 is responsible for charging the rest of the nodes. When r_1 and r_4 return back to their respective home stations, the volumes of residual batteries are 771 J and 536 J, respectively. With PDA, itineraries r_2 and r_3 are chosen: r_2 is responsible for charging s_6, s_7, s_8, and s_9, while r_3 is responsible for charging the rest of the nodes. When r_2 and r_3 return to their respective home stations, the volumes of residual batteries are 963 J and 42 J, respectively. The total charging times of OPT and PDA are 219 and 347 s, respectively. We see that PDA incurs more loss-energy than OPT, but also leads to less movement-energy than OPT.

7 Simulation Results

In this section, we evaluate the performance of the proposed algorithms through extensive simulations.

7.1 Simulation Setup

Similar to existing works [13], [16], [17], we set $a = 1$ and $b = 10$ in the wireless power transfer model (Eq. (2)). The transmission power P of each mobile charger is set to 100. The volume of energy required by each device, E, is 0.5. The movement-energy c_i of each itinerary r_i is uniformly distributed within the range $[3{,}000, 8{,}000]$. The charging time capacity T_i of each itinerary r_i is uniformly distributed within the range $[30, 80]$. The time t_{ij} for a charger r_i to charge a device s_j to its full requirement is uniformly distributed within the range $[1, 10]$. The loss-energy f_{ij} during

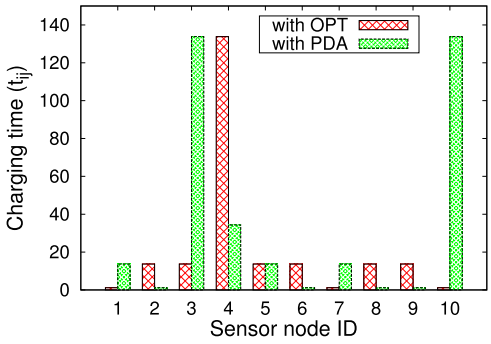

Fig. 8. Charging time of 10 sensor nodes when they are placed as shown in Fig. 6b. The total charging times with OPT and PDA are 219 and 347, respectively. We find that PDA incurs more loss-energy than OPT although it leads to less movement-energy than OPT.

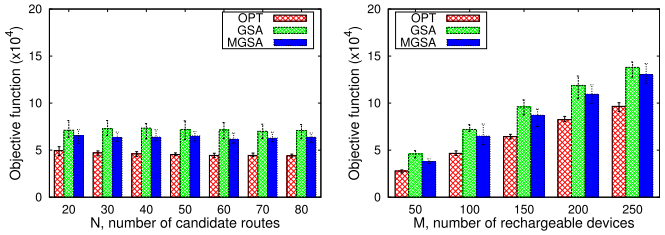

(a) Varying N under fixed $M = 100$ (b) Varying M under fixed $N = 40$

Fig. 9. Simulation results for ISCA.

r_i charges s_j to its full requirement can be obtained by observing $f_{ij} = Pt_{ij} - E$. The default number N of candidate itineraries is 40. The default number M of rechargeable devices is 100.

We also introduce a heuristic algorithm for ISCA-MP: Multipick-oriented Modified GSA, or MMGSA for short, for performance comparison. The main differences between MMGSA and MGSA include the following: (i) we no longer need to maintain $\mathcal{R}'$; (ii) g_{ij} is defined over $\mathcal{R} \setminus \{i\}$, because each selected itinerary can be reused, i.e., $\forall r_i \in \mathcal{R}, \forall s_j \in \mathcal{S} \setminus \mathcal{S}'$, we let

$$g_{ij} = \frac{1}{|\mathcal{R} \setminus (\mathcal{R}' \cup \{i\})|} \sum_{k \in \mathcal{R} \setminus (\mathcal{R}' \cup \{i\})} f_{kj};$$

and (iii) when $r_{i'}$ is selected (line 11 in Alg. MGSA), $y_{i'}$ is updated to $y_{i'} + 1$.

7.2 Simulation Results

We present and analyse simulation results in this subsection.

Fig. 9 shows the comparison results of running OPT, GSA, and MGSA for the ISCA problem. In general, we find that though GSA has a theoretic performance guarantee, it performs worse than MGSA in all settings. More specifically, in Fig. 9a, GSA is 161 percent at most and 157 percent on average of OPT, while MGSA is 145 percent at most and 139 percent on average of OPT. However, GSA never performs worse than its bound, i.e., $O(\ln M)$. In Fig. 9a, when the number of candidate itineraries increases, the average performance of all three algorithms improves very slightly, implying that $N = 20$ itineraries may be sufficient for the setting. In Fig. 9b, when the number of energy-hungry devices increases, the energy cost of all three algorithms increases; this is reasonable, since more devices require more itineraries (i.e., more movement-energy) and associations (i.e., more loss-energy).

Fig. 10 shows the comparison results of running OPT, PDA, and MMGSA for the ISCA-MP problem. We make

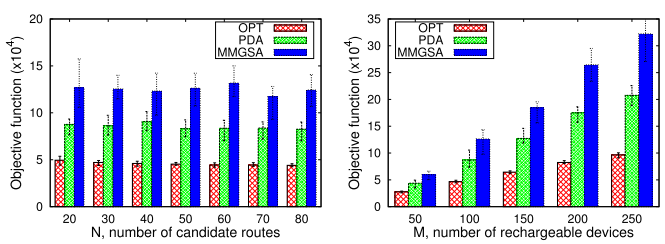

(a) Varying N under fixed $M = 100$ (b) Varying M under fixed $N = 40$

Fig. 10. Simulation results for ISCA-MP.

M \ N	20	30	40	50	60	70	80
50	1.52	1.62	1.66	1.61	1.71	1.76	1.76
100	1.43	1.55	1.59	1.59	1.61	1.58	1.61
150	1.40	1.41	1.57	1.53	1.60	1.53	1.62

(a) The $\frac{GSA}{OPT}$ ratio for ISCA in simulations

M \ N	20	30	40	50	60	70	80
50	1.56	1.53	1.57	1.73	1.59	1.56	1.63
100	1.77	1.83	1.97	1.83	1.88	1.89	1.87
150	1.86	2.00	1.97	2.01	2.04	2.06	2.03

(b) The $\frac{PDA}{OPT}$ ratio for ISCA-MP in simulations

Fig. 11. The theoretical approximation ratios of GSA for ISCA and PDA for ISCA-MP are $O(\ln M)$ and 10, respectively. We see that the practical performance of GSA and PDA is better than numerical analysis. (For reference, $\ln 50 = 3.91, \ln 100 = 4.61$, and $\ln 150 = 5.01$.)

similar observations as in Fig. 9. One thing worth mentioning is that, unlike in Fig. 9, PDA performs much better than MMGSA. For example, in Fig. 10a, PDA is 197 percent at most and 186 percent on average of OPT, while MMGSA is 297 percent at most and 273 percent on average of OPT. This is because, PDA employs primal-dual schema to cope with the intractability of ISCA-MP, while MMGSA greedily picks charging itineraries. We also find that for the same setting (e.g., Fig. 9a and Fig. 10a), PDA performs better than GSA. The main reason is that PDA can use each itinerary multiple times, giving it more opportunities to optimize the objection function.

As we claimed in Section 5.6, though the approximation ratios of GSA and PDA are $O(\ln M)$ and 10, respectively, in reality, they work much better than the bounds. Fig. 11 confirms our claim. Fig. 11 shows the $\frac{GSA}{OPT}$ ratio for ISCA and the $\frac{PDA}{OPT}$ ratio for ISCA-MP under varying numbers of charging itineraries and rechargeable devices. For GSA, the theoretical approximation ratio is $O(\ln M)$ (for reference, ln50 =3.91, ln100 = 4.61, and ln150 = 5.01), while the $\frac{GSA}{OPT}$ ratio in simulations is no more than 1.76. Similarly, for PDA, the theoretical approximation ratio is 10, while the $\frac{PDA}{OPT}$ ratio in simulations is no more than 2.06. We also have examined extremely large instances of ISCA and ISCA-MP, in which the results are always consistent with our numerical analysis.

All of the proposed algorithms are very time-efficient in our simulations. For example, when $N = 80$ and $M = 100$, the running time of GSA, MGSA, PDA, and MMGSA are 0.17, 1.36, 11.68, and 2.68, respectively. We note that MGSA achieves a better solution than GSA for ISCA, but that its running time is slightly longer. Similarly, MMGSA achieves a worse solution than PDA for ISCA-MP, but its running time is shorter.

Key observations are summarized as follows. First, although GSA has theoretical performance guarantee, MGSA performs better than GSA for ISCA. Second, PDA employs the primal-dual schema to cope with the intractability of ISCA-MP, and thus gives better results than MMGSA. Third, for the same problem setting, PDA achieves better results than GSA; this is because PDA can use each itinerary multiple times, giving it more opportunities to optimize the objective function. Last, all of the proposed algorithms are time-efficient. GSA is within 176 percent of OPT in ISCA, and PDA is within 206 percent of OPT in ISCA-MP throughout the simulations, validating our theoretical analyses.

8 Conclusion

The explosive growth of mobile devices and their increasing functionality have made them a vital part of our lives. Determining how to replenish these energy-hungry devices so as to prolong their lifespans and support sustainable operations is of the utmost importance. In this paper, we consider the wireless charging service provision using mobile chargers and study the itinerary selection and charging association problem, i.e., the ISCA problem. We prove that ISCA is NP-complete. For the case in which each itinerary can only be used once, we devise an $O(\ln M)$-approximation algorithm and a practical heuristic algorithm; for the case in which each itinerary can be used multiple times, we design a 10-approximation algorithm based on the Primal-Dual schema. Real field experiments and extensive evaluations have confirmed the performance of our algorithms compared with the optimal fractional solutions.

There are a number of research directions we plan to study following this work. The first is to investigate the case where candidate charging itineraries are not fixed. The second is to incorporate radiation safety into our charging framework and make sure that no physical point receives an electromagnetic radiation that is higher than the safety threshold for human beings.

Acknowledgments

This work was supported in part by NSFC (61502224, 61472181, 61472185, 61321491), China Postdoctoral Science Foundation (2015M570434, 2016T90444), CCF-Tencent Open Research Fund (AGR20160104), Jiangsu NSF (BK20151392, BK20151390), and Collaborative Innovation Center of Novel Software Technology and Industrialization.

References

[1] A. Kansal, J. Hsu, S. Zahedi, and M. B. Srivastava, "Power management in energy harvesting sensor networks," *ACM Trans. Embedded Comput. Syst.*, vol. 6, Sep. 2007, Art. no. 32.

[2] A. Dunkels, F. Österlind, and Z. He, "An adaptive communication architecture for wireless sensor networks," in *Proc. 5th Int. Conf. Embedded Netw. Sensor Syst.*, 2007, pp. 335–349.

[3] B. Tong, G. Wang, W. Zhang, and C. Wang, "Node reclamation and replacement for long-lived sensor networks," *IEEE Trans. Parallel Distrib. Syst.*, vol. 22, no. 9, pp. 1550–1563, Sep. 2011.

[4] A. Kurs, A. Karalis, R. Moffatt, J. D. Joannopoulos, P. Fisher, and M. Soljačić, "Wireless power transfer via strongly coupled magnetic resonances," *Science*, vol. 317, no. 5834, pp. 83–86, 2007.

[5] K. Kang, Y. S. Meng, J. Bréger, C. P. Grey, and G. Ceder, "Electrodes with high power and high capacity for rechargeable lithium batteries," *Science*, vol. 311, no. 5763, pp. 977–980, 2006.

[6] Androidcentral, (2015, Jul.). [Online]. Available: http://www.androidcentral.com/these-android-phones-can-handle-wireless-charging/

[7] Tesla motors, (2015, Jul.). [Online]. Available: http://www.teslamotors.com/

[8] SHARP, (2015, Jul.). [Online]. Available: http://www.friendsofcrc.ca/Projects/SHARP/sharp.html

[9] Wireless charging market, (2015, Jul.). [Online]. Available: http://www.marketsandmarkets.com/PressReleases/wireless-charging.asp

[10] Y. Peng, Z. Li, W. Zhang, and D. Qiao, "Prolonging sensor network lifetime through wireless charging," in *Proc. IEEE 31st IEEE Real-Time Syst. Symp.*, 2010, pp. 129–139.

[11] Y. Shi, L. Xie, Y. Hou, and H. Sherali, "On renewable sensor networks with wireless energy transfer," in *Proc. IEEE INFOCOM* 2011, pp. 1350–1358.

[12] L. Xie, Y. Shi, Y. T. Hou, W. Lou, H. D. Sherali, and S. F. Midkiff, "On renewable sensor networks with wireless energy transfer: The multi-node case," in *Proc. 9th Annu. IEEE Commun. Soc. Conf. Sensor Mesh Ad Hoc Commun. Netw.*, 2012, pp. 10–18.

[13] L. Fu, P. Cheng, Y. Gu, J. Chen, and T. He, "Minimizing charging delay in wireless rechargeable sensor networks," in *Proc. IEEE INFOCOM* 2013, pp. 2922–2930.
[14] S. Zhang, J. Wu, and S. Lu, "Collaborative mobile charging," *IEEE Trans. Comput.*, vol. 64, no. 3, pp. 654–667, Mar. 2015.
[15] S. Zhang, Z. Qian, F. Kong, J. Wu, and S. Lu, "P^3: Joint optimization of charger placement and power allocation for wireless power transfer," in *Proc. IEEE INFOCOM* 2015, pp. 2344–2352.
[16] S. He, J. Chen, F. Jiang, D. K. Yau, G. Xing, and Y. Sun, "Energy provisioning in wireless rechargeable sensor networks," in *Proc. IEEE INFOCOM* 2011, pp. 2006–2014.
[17] H. Dai, Y. Liu, G. Chen, X. Wu, and T. He, "Safe charging for wireless power transfer," in *Proc. IEEE INFOCOM* 2014, pp. 1105–1113.
[18] Z. Li, Y. Peng, W. Zhang, and D. Qiao, "Study of joint routing and wireless charging strategies in sensor networks," in *Proc. 5th Int. Conf. Wireless Algorithms Syst. Appl.* 2010, pp. 125–135.
[19] L. He, et al., "Esync: An energy synchronized charging protocol for rechargeable wireless sensor networks," in *Proc. 15th ACM Int. Symp. Mobile ad hoc Netw. Comput.*, 2014, pp. 247–256.
[20] M. Zhao, J. Li, and Y. Yang, "A framework of joint mobile energy replenishment and data gathering in wireless rechargeable sensor networks," *IEEE Trans. Mobile Comput.*, vol. 13, no. 12, pp. 2689–2705, Dec. 2014.
[21] C. Wang, J. Li, F. Ye, and Y. Yang, "NETWRAP: An NDN based real-timewireless recharging framework for wireless sensor networks," *IEEE Trans. Mobile Comput.*, vol. 13, no. 6, pp. 1283–1297, Jun. 2014.
[22] T. H. Cormen, C. E. Leiserson, R. L. Rivest, and C. Stein, *Introduction to Algorithms*. Cambridge, MA, USA: MIT Press, 2001.
[23] B. Tong, Z. Li, G. Wang, and W. Zhang, "How wireless power charging technology affects sensor network deployment and routing," in *Proc. IEEE 30th Int. Conf. Distrib. Comput. Syst.*, 2010, pp. 438–447.
[24] H. Dai, Y. Liu, A. X. Liu, L. Kong, G. Chen, and T. He, "Radiation constrained wireless charger placement," in *Proc. IEEE INFOCOM*, 2016, pp. 1–9.
[25] S. Nikoletseas, T. P. Raptis, and C. Raptopoulos, "Low radiation efficient wireless energy transfer in wireless distributed systems," in *Proc. IEEE 35th Int. Conf. Distrib. Comput. Syst.*, Jun. 2015, pp. 196–204.
[26] Y. Shu, H. Yousefi, P. Cheng, J. Chen, Y. Gu, T. He, and K. Shin, "Near-optimal velocity control for mobile charging in wireless rechargeable sensor networks," *IEEE Trans. Mobile Comput.*, vol. 15, no. 7, pp. 1699–1713, Jul. 2016.
[27] L. Fu, L. He, P. Cheng, Y. Gu, J. Pan, and J. Chen, "ESync: Energy synchronized mobile charging in rechargeable wireless sensor networks," *IEEE Trans. Veh. Technol.*, vol. 65, no. 9, pp. 7415–7431, Sept. 2016.
[28] W. Xu, W. Liang, X. Lin, and G. Mao, "Efficient scheduling of multiple mobile chargers for wireless sensor networks," *IEEE Trans. Veh. Technol.*, vol. 65, no. 9, pp. 7670–7683, Sept. 2016.
[29] S. Nikoletseas, T. P. Raptis, and C. Raptopoulos, "Interactive wireless charging for energy balance," in *Proc. IEEE 36th Int. Conf. Distrib. Comput. Syst.*, Jun. 2016, pp. 262–270.
[30] C. Wang, J. Li, Y. Yang, and F. Ye, "A hybrid framework combining solar energy harvesting and wireless charging for wireless," in *Proc. IEEE INFOCOM*, 2016, pp. 1–9.
[31] L. Chen, S. Lin, and H. Huang, "Charge me if you can: Charging path optimization and scheduling in mobile networks," in *Proc. 17th ACM Int. Symp. Mobile Ad Hoc Netw. Comput.*, 2016, pp. 101–110.
[32] G. B. Dantzig and J. H. Ramser, "The truck dispatching problem," *Manage. Sci.*, vol. 6, no. 1, pp. 80–91, 1959.
[33] V. V. Vazirani, *Approximation Algorithms*. Berlin, Germany: Springer, 2003.
[34] Powercast, (2015, Jul.). [Online]. Available: http://www.powercastco.com/
[35] PuLP, (2015, Jul.). [Online]. Available: https://pythonhosted.org/PuLP/

Sheng Zhang received the BS and PhD degrees from Nanjing University, in 2008 and 2014, respectively. Now he is an assistant professor with Nanjing University. He is also a member of the State Key Lab. for Novel Software Technology. His research interests include cloud computing and mobile networks. His publications appeared in the *IEEE Transactions on Mobile Computing*, the *IEEE Transactions on Parallel and Distributed Systems*, the *IEEE Transactions on Computers*, ICDCS, INFOCOM, and ACM MobiHoc. He received the Best Paper Runner-Up Award from IEEE MASS 2012. He is a member of the IEEE.

Zhuzhong Qian received the PhD degree from Nanjing University, in 2007. He is an associate professor in the Department of Computer Science and Technology, Nanjing University. His current research interests include distributed systems and data center networking. He has published more than 40 papers in referred journals and conferences, including the *IEEE Transactions on Parallel and Distributed Systems*, INFOCOM, and IPDPS. He is a member of the IEEE.

Jie Wu (F'09) is the chair and a Laura H. Carnell professor in the Department of Computer and Information Sciences, Temple University. He is also an intellectual ventures endowed visiting chair professor in the National Laboratory for Information Science and Technology, Tsinghua University. Prior to joining Temple University, he was a program director of the National Science Foundation and was a distinguished professor with Florida Atlantic University. His current research interests include mobile computing and wireless networks, routing protocols, cloud and green computing, network trust and security, and social network applications. He regularly publishes in scholarly journals, conference proceedings, and books. He serves on several editorial boards, including the *IEEE Transactions on Service Computing* and the *Journal of Parallel and Distributed Computing*. He was general co-chair/chair for IEEE MASS 2006, IEEE IPDPS 2008, IEEE ICDCS 2013, and ACM MobiHoc 2014, as well as program co-chair for IEEE INFOCOM 2011 and CCF CNCC 2013. He was an IEEE Computer Society distinguished visitor, ACM distinguished speaker, and chair for the *IEEE Technical Committee on Distributed Processing*. He received the 2011 China Computer Federation (CCF) Overseas Outstanding Achievement Award. He is a CCF distinguished speaker and a fellow of the IEEE.

Fanyu Kong received the BS and MS degrees from Nanjing University, in 2013 and 2016, respectively. He is now with Ant Financial, China. His research interests include load balancing and failure monitoring in public clouds via openstack.

Sanglu Lu received the BS, MS, and PhD degrees from Nanjing University, in 1992, 1995, and 1997, respectively, all in computer science. She is currently a professor in the Department of Computer Science and Technology, Nanjing University and the State Key Laboratory for Novel Software Technology. Her research interests include distributed computing, wireless networks, and pervasive computing. She has published more than 80 papers in referred journals and conferences in the above areas. She is a member of IEEE.